Structural relaxation of poly(γ-benzyl-L-glutamate)

F. Romero Colomer* and J. L. Gómez Ribelles†

**Applied Physics Department and †Laboratory of Thermodynamics and Physical Chemistry, Universidad Politécnica de Valencia, PO Box 22012, 46071 Valencia, Spain*

(Received 2 August 1988; revised 7 November 1988; accepted 16 November 1988)

A structural relaxation process similar to that in amorphous polymers has been found in poly(γ-benzyl-L-glutamate). Its kinetics has been determined by differential scanning calorimetry and modelled using a phenomenological model. The parameters characterizing the shape and temperature dependence of the distribution of recovery times have been compared with those describing the dielectric relaxation process, occurring in the same range of temperatures. The process is ascribed to conformational rearrangements of the side chains and is responsible for the glass transition and the WLF behaviour of the dielectric relaxation described in the literature.

(Keywords: poly(γ-benzyl-L-glutamate); glass transition; structural relaxation; dielectric relaxation)

INTRODUCTION

The main chain of poly(γ-benzyl-L-glutamate) (PBLG) in the solid state adopts an α-helicoidal conformation when the polymer is obtained by casting from a helicogenic solvent[1,2]. The α-helices are ordered in a hexagonal lattice forming a paracrystalline phase in which the side chains occupy the inter-helix space[1–7]. No definite structure has been detected in the side chains, and a liquid-like behaviour has been proposed for them when considered as a separate phase from the helices[8–10].

Several properties, which usually characterize amorphous materials, are present in PBLG and are ascribed to molecular movements of the side groups; thus a mechanical and dielectric relaxation process has been observed at temperatures above ambient. The dependence of the temperature of the maximum with frequency corresponds to the Williams–Landel–Ferry (WLF) behaviour, which is found in the α-relaxation of amorphous polymers and other glass-forming materials and is associated with the glass transition. This relaxation has been studied extensively and is assigned to the onset of side-chain movements when the temperature increases[11–13]. A change in the slope of the specific volume *versus* temperature plot at 15°C has also been reported and related to a corresponding change of slope of the inter-helix distance *versus* temperature plot[7,14]. Both experimental facts lead to the idea of the existence of a glass transition in the side-chain phase of the polymer.

The glass transition in amorphous polymers reflects the transition between the liquid state, in which the material is in thermodynamic equilibrium, and the glassy state, not in equilibrium. A sudden change in the temperature of the polymer is followed by a relaxation process in which the specific volume, enthalpy and other physical properties attain new equilibrium values. This process is known as a structural relaxation process. When the recovery time of the structural relaxation is much smaller than the experimental time, the observed states of the material are always in equilibrium states, and the polymer is said to be in the liquid state. When the recovery time is of the order of magnitude of the experimental times, states not in equilibrium are detected and the polymer is said to be in the glassy state. The transition between liquid and glassy states occurs in the range of temperatures in which the structural recovery time (which increases when the temperature decreases) attains the order of magnitude of the experimental times.

The glass transition is closely related to the structural relaxation. The aim of this work is to prove that the origin of the transition found in PBLG is a structural relaxation process similar to that observed in amorphous polymers, characterizing this process by means of differential scanning calorimetry. The dielectric relaxation spectrum will also be characterized in order to establish a relationship between dielectric and structural relaxation processes.

EXPERIMENTAL

The film (30 μm thick) of PBLG with a degree of polymerization of 1820, prepared by casting from dichloromethane solution, was kindly supplied by Professor T. Nakagawa from Meiji University, Japan. The sample was dried *in vacuo* for several days before measurements were carried out. The i.r. spectrum measured with a Perkin–Elmer 781 infra-red spectrometer is characteristic of the α-helical conformation in the main chain.

Dielectric measurements were carried out in a GenRad 1620 A capacitor bridge, in the range of frequencies between 60 Hz and 100 kHz. The sample used was gold metallized.

The sample used in calorimetric experiments, weight 8.90 mg, was sealed in an aluminium pan. The same sample was used in all the measurements. A Perkin–Elmer DSC 4 calorimeter with a data station model 3600 was used. The thermal history of the experiments, carried out in the calorimeter, started with annealing at 40°C

0032-3861/89/050849-07$03.00

for 10 min to ensure that the sample was in equilibrium and also to eliminate the effect of previous thermal histories. The sample was then cooled at 40°C min^{-1} until the ageing temperature T_a, held at this temperature for an ageing time t_a, cooled again at 40°C min^{-1} to −50°C and then heated at 20°C min^{-1} to 40°C. Data were collected only on heating. The specific heat was calculated by comparison with the result of a measuring scan on a sapphire standard sample. The $C_p(T)$ curve measured after a thermal history with $t_a \neq 0$ will be called an ageing scan and the one with $t_a = 0$ a reference scan.

RESULTS AND DISCUSSION

Figure 1 presents an example of the specific heat curves measured after ageing and a reference scan. The curves are similar to those found in amorphous polymers. The glass transition appears in the range of temperatures between −10 and 40°C. The glass transition temperature of ~26°C, calculated by the intersection of the enthalpy *versus* temperature curves in the liquid and glassy states, is higher than the value reported by dilatometric experiments*, as happens in other polymers[15,16]. The increment of enthalpy suffered by the polymer during the isothermal stage of the thermal history (Δh_a) was calculated from the difference between the ageing and reference scans as described in ref. 15. The evolution of the enthalpy with ageing time at $T_a = 10$°C and $T_a = -5$°C is represented in *Figure 2*. Again a plot similar to that for amorphous polymers is obtained, showing the non-equilibrium behaviour of the polymer at these temperatures. The values of Δh_a are practically independent of the ageing temperature, which can be attributed to the ageing time range used. The influence of T_a will be more apparent at higher ageing times[17].

Several phenomenological models have been proposed for the structural relaxation, based on the idea of a distribution of recovery times that is both temperature- and structure-dependent[18–21].

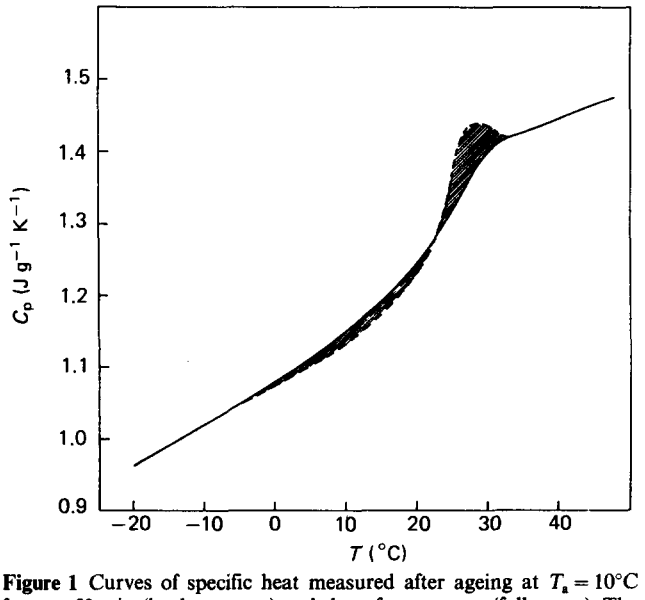

Figure 1 Curves of specific heat measured after ageing at $T_a = 10$°C for $t_a = 50$ min (broken curve) and the reference scan (full curve). The shaded area equals the increment of enthalpy of the sample during the isothermal stage

*The onset glass transition temperature is 17°C, closer to the dilatometric one

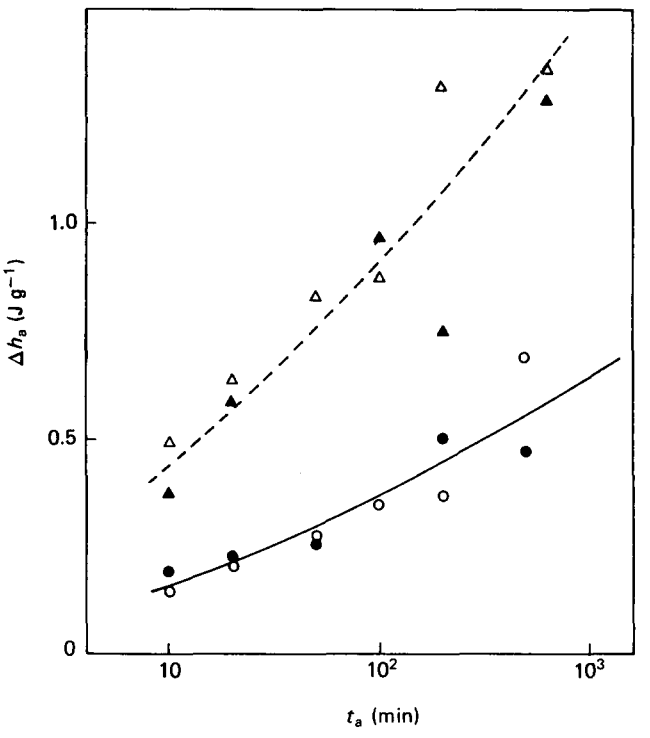

Figure 2 Experimental enthalpy increment due to ageing at $T_a = 10$°C (○) and $T_a = -5$°C (●), and the model predictions for the same thermal histories, $T_a = 10$°C (△) and $T_a = -5$°C (▲). There are no significant differences between both T_a in either the experimental behaviour or the model predictions. The full curve characterizes the experimental behaviour and the broken curve the model predictions

The isothermal enthalpy recovery is described by means of a decay function[18–21] following the Williams–Watts[22] form:

$$\phi(t_1, t_a) = \exp\left[-\left(\int_{t_1}^{t_a} \frac{dt}{\tau}\right)^{\beta}\right] \quad (1)$$

where τ is a function of the temperature and of the separation from equilibrium, the latter usually represented by means of the fictive temperature, T_f. Several expressions have been tested for $\tau(T, T_f)$[18–20,23]. In this work, we will use the one recently proposed by Hodge[20] and deduced from the Adam and Gibbs[24] theory:

$$\tau = A \exp\left(\frac{D}{RT(1 - T_2/T_f)}\right) \quad (2)$$

A, D and T_2 are three adjustable parameters, which also define the values of τ corresponding to equilibrium ($T = T_f$):

$$\tau^{eq} = \exp\left(\frac{-D}{R(T - T_2)}\right) \quad (3)$$

The parameter β in (1) defines the width of the distribution of recovery times, so a total of four parameters characterize the structural relaxation process.

A reference temperature T_R is defined in this work as the temperature at which the value of τ^{eq} equals 1 s, so:

$$A = \exp\left(\frac{-D}{R(T_R - T_2)}\right) \quad (4)$$

T_R is a more useful parameter than A for the interpretation of the results because it is close to the experimental temperature range.

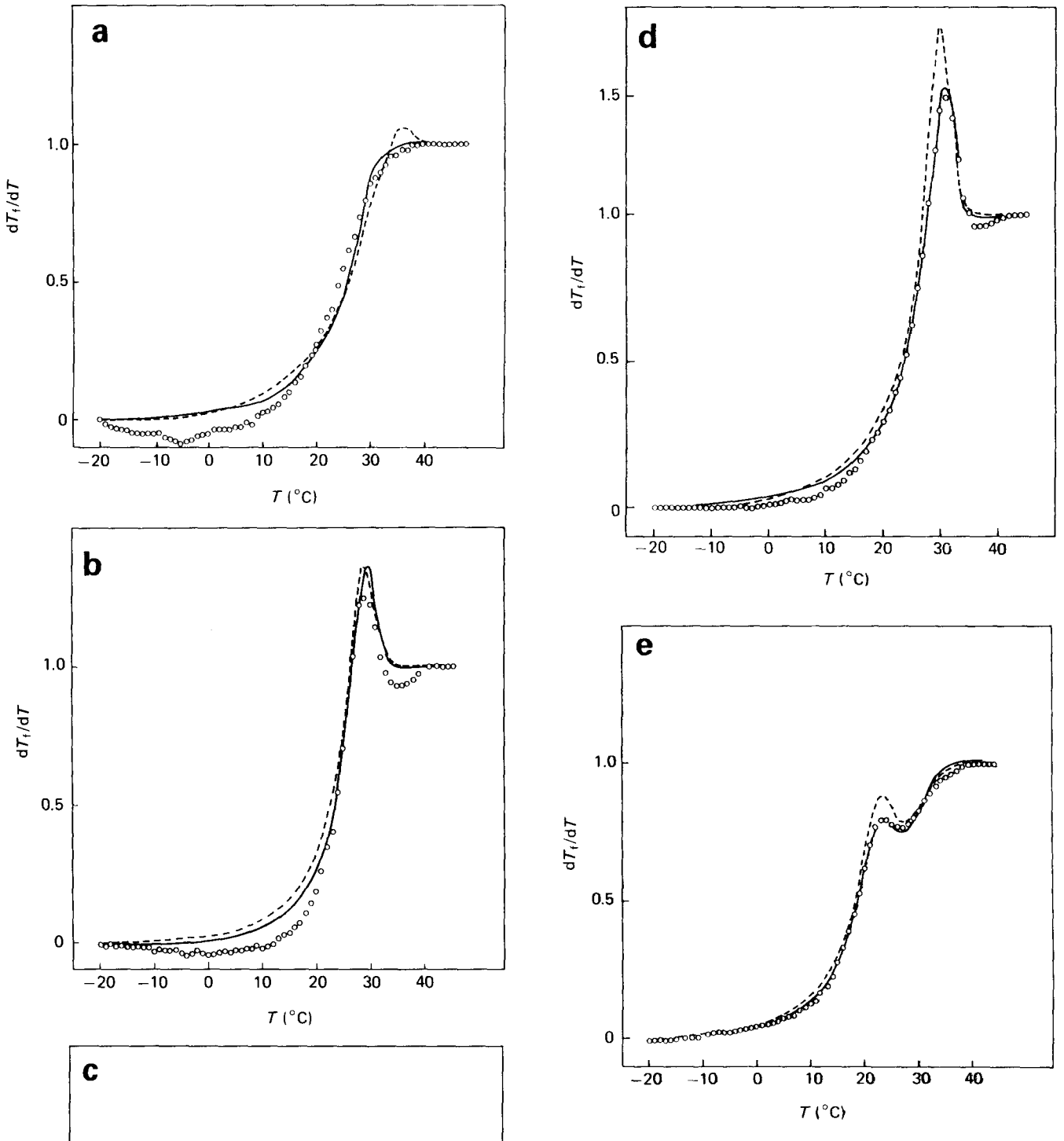

Figure 3 Experimental curves of dT_f/dT for several thermal histories. The full curve represents the best fit found with the model. The broken curve represents the best adjustment found keeping fixed the parameters $T_R = 32.62°C$, $T_2 = -41°C$ and $D = 6$ kcal mol^{-1}. (a) Result without ageing ($t_a = 0$); (b) $T_a = 10°C$, $t_a = 100$ min; (c) $T_a = -5°C$, $t_a = 100$ min; (d) $T_a = 10°C$, $t_a = 500$ min; (e) $T_a = -5°C$, $t_a = 500$ min

The experimental data are usually represented in terms of the fictive temperature. Its derivative with respect to temperature acts as a normalized specific heat:

$$\frac{dT_f}{dT} = \frac{(C_p - C_{pg})(T)}{(C_{pl} - C_{pg})(T_f)}$$

where $C_{pl}(T)$ and $C_{pg}(T)$ are the specific heats of the liquid and the glass respectively.

Figure 3 shows the dT_f/dT curves calculated from the specific heat curves measured after ageing at 10°C and

−5°C for times ranging between 100 and 500 min. For the ageing temperature of 10°C the peak in dT_f/dT overlaps the high-temperature side of the transition and shifts towards high temperatures when the ageing time increases, as expected for an ageing temperature close to T_g. The curves measured after ageing at −5°C show a peak at lower temperatures within the range of the transition. These peaks reflect an increase of the enthalpy at those temperatures, moving in the opposite direction to that of approaching equilibrium, and have been related to the memory effect[25].

The thermal histories of the experiments have been computer-simulated using the expressions (1) and (2). The cooling or heating stages were substituted in the computer program by a series of steps of 1°C and isothermal stages leading to the same average thermal history. The four parameters of the model were adjusted to the experimental results using the Nedler and Mead method[26].

A strong correlation between the four parameters of the model was found, so several ensembles of values of the parameters fit the experimental curve with similar accuracy. This has been detected in other models and polymers[19,27].

In this work the fitting procedure was the following. The curves measured after thermal histories with the highest ageing time at 10°C and −5°C were fitted with fixed values of the parameter D looking for the best adjustment when changing the other three parameters. On both series of curves a systematic dependence of T_2 with D was found. The value of T_R is nearly independent of D and β changes slightly (more clearly for $T_a = -5$°C). The results are shown in *Table 1*. It is interesting to note that different pairs of values of D and T_2 lead to similar curves of τ^{eq} *versus* $1/T$ in the experimental range of temperatures of the ageing experiments.

A value of $D = 6$ kcal mol^{-1} is the one which best reproduces the low-temperature ageing peaks at $T_a = -5$°C with a reasonable fit of the curves as a whole. It was thus selected in the fit of the curves corresponding to the rest of the ageing times. The values of the parameters are given in *Table 2* and in *Figure 3* the calculated curves are represented by full curves.

The systematic changes of the parameters of the model have also been reported in other polymers in different phenomenological models[27,28], and it is difficult to give an interpretation of this within the framework of the theory. Nevertheless the equilibrium curves corresponding to the parameters obtained for different thermal histories fall in a narrow strip in the diagram of log τ^{eq} *versus* $1/T$ (*Figure 4*). The curve with parameters $D = 6$ kcal mol^{-1}, $T_2 = -41$°C and $T_R = 32.62$°C can be taken as an average. When the different curves are fitted with these values of D, T_2 and T_R, a value of β ranging between 0.25 and 0.36 is found (*Table 3*) with an acceptable fit to the experimental curves (broken curves in *Figure 3*). The dependence of β on the thermal history cannot be avoided without an important separation of the calculated curve from the experimental points.

It can be concluded that the τ^{eq} curve marked in *Figure 3* by a broken curve and a value of β ranging

Table 1 Parameters calculated at a single t_a of 500 min ($\hat{\sigma}^2$ is the residual error variance)

T_a (°C)	t_a (min)	D (kcal mol^{-1})	T_R (°C)	T_2 (°C)	β	$\hat{\sigma}^2$
10	500	3	35.0	−23.3	0.23	0.00331
10	500	4	36.2	−29.0	0.22	0.00245
10	500	5	35.0	−34.5	0.24	0.00110
10	500	6	34.7	−38.4	0.24	0.00007
10	500	7	34.6	−43.8	0.25	0.00005
10	500	8	34.5	−49.2	0.25	0.00006
−5	500	5	31.7	−30.3	0.27	0.00410
−5	500	6	32.4	−36.6	0.30	0.00145
−5	500	7	31.6	−43.3	0.31	0.00113
−5	500	8	31.9	−50.2	0.32	0.00095
−5	500	9	32.1	−56.7	0.33	0.00079

Table 2 Parameters calculated with a fixed value of $D = 6$ kcal mol^{-1}

T_a (°C)	t_a (min)	D (kcal mol^{-1})	T_R (°C)	T_2 (°C)	β	$\hat{\sigma}^2$
–	0	6	28.6	−24.4	0.22	0.00376
10	10	6	30.6	−35.0	0.34	0.00482
10	20	6	32.7	−40.2	0.33	0.00440
10	50	6	31.3	−40.9	0.29	0.00097
10	100	6	32.5	−37.6	0.30	0.00415
10	200	6	34.2	−42.6	0.25	0.00094
10	500	6	34.7	−38.4	0.24	0.00007
−5	10	6	30.8	−39.5	0.33	0.00105
−5	20	6	31.0	−42.4	0.31	0.00079
−5	100	6	31.0	−38.9	0.31	0.00168
−5	200	6	31.1	−36.3	0.33	0.00311
−5	500	6	32.4	−36.6	0.30	0.00145

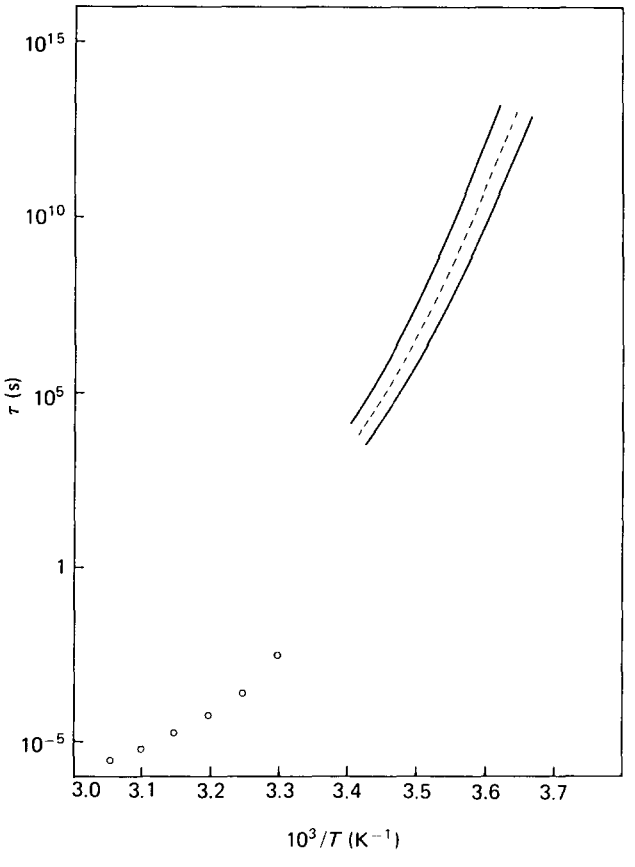

Figure 4 Equilibrium values of τ^{eq}. The open circles are values found in dielectric measurements, $\tau^{eq} = 1/\omega_m$. The values found in calorimetric experiments for the different thermal histories are between the two full curves. The broken curve is the average curve used for the last adjustment (see text)

between 0.25 and 0.36 gives a good description of the structural relaxation of PBLG. These values will be compared below with the ones found in the dielectric relaxation.

The values of Δh_a predicted by the model are higher than observed experimentally (*Figure 2*). In the model predictions the influence of T_a on Δh_a within the experimental ageing times is small, as happens with the experimental values.

The dielectric relaxation spectrum of PBLG shows a prominent peak at temperatures above the glass transition temperature. *Figure 5* shows the ε'' (imaginary part of the complex dielectric permittivity) curves determined in the range of temperatures between 15.5 and 74.5°C. The Williams–Watts[22] decay function can also be used to model the dielectric relaxation in equilibrium conditions:

$$\phi(t) = \exp[-(t/\tau)^{\beta}] \quad (5)$$

and the complex dielectric permittivity can be calculated by means of:

$$\frac{\varepsilon^*(\omega) - \varepsilon_\infty}{\varepsilon_0 - \varepsilon_\infty} = \int_{-\infty}^{\infty} \left(-\frac{d\phi(t)}{dt}\right) \exp(-i\omega t)\, dt \quad (6)$$

As in structural relaxation, the single parameter β defines the shape of the distribution of relaxation times. This distribution and the plot of $\varepsilon''/(\varepsilon_0 - \varepsilon_\infty)$ vs. $\log(\omega\tau_0)$ or $\varepsilon''/\varepsilon''_m$ vs. $\log(f/f_m)$ are only dependent on the value of β. A series of those curves were determined by Williams *et al.*[29] A master curve $\varepsilon''/\varepsilon''_m$ vs. $\log(f/f_m)$ obtained from our results is represented in *Figure 6*. The superposition is good at the maximum and on the high-frequency side of the curves, but scattering is marked on the low-frequency side. On this plot, the curve corresponding to the model with $\beta = 0.35$ is represented. The agreement between the model and the experiment is excellent on the high-frequency side of the master curve. The value of β is very close to that found in the structural relaxation process, indicating that the width of the relaxation time spectrum which governs both processes is very similar.

The maximum of the model curves appears at a frequency slightly below $1/\tau_0$. Nevertheless the difference is small and a good approximation to τ_0, in order to compare it with the equilibrium recovery times of the structural relaxation, is $\tau_0 = 1/\omega_m = 1/2\pi f_m$, f_m being the frequency at which ε'' goes through the maximum.

In *Figure 4* the values of $\log(\tau_0)$ for the different temperatures are represented. The characteristic curvature of this plot, corresponding to WLF or Vogel behaviour, is apparent. As found in amorphous polymers, there is no coincidence between the equilibrium recovery times determined by means of the dielectric and structural methods; nevertheless the range of temperatures is very different in this experiment and low-frequency dielectric or mechanical measurements would be necessary to reach further conclusions.

The nature of the glass transition in amorphous polymers can be understood by the application of statistical thermodynamic theories. The thermodynamic variables of a liquid in equilibrium are determined by the number and energy of the possible configurations of the chain molecules, through the partition configurational function. The number of ways in which the chain molecules can be packed in the bulk phase diminishes

Table 3 The β parameters that give the best fits using the average τ curves

T_a (°C)	t_a (min)	β	$\hat{\sigma}^2$	T_a (°C)	t_a (min)	β	$\hat{\sigma}^2$
10	10	0.35	0.00565	−5	10	0.32	0.00281
10	20	0.33	0.00474	−5	20	0.28	0.00268
10	50	0.30	0.00095	−5	50	0.35	0.00371
10	100	0.30	0.00623	−5	100	0.31	0.00171
10	200	0.26	0.00156	−5	200	0.32	0.00374
10	500	0.25	0.00642	−5	500	0.29	0.00227

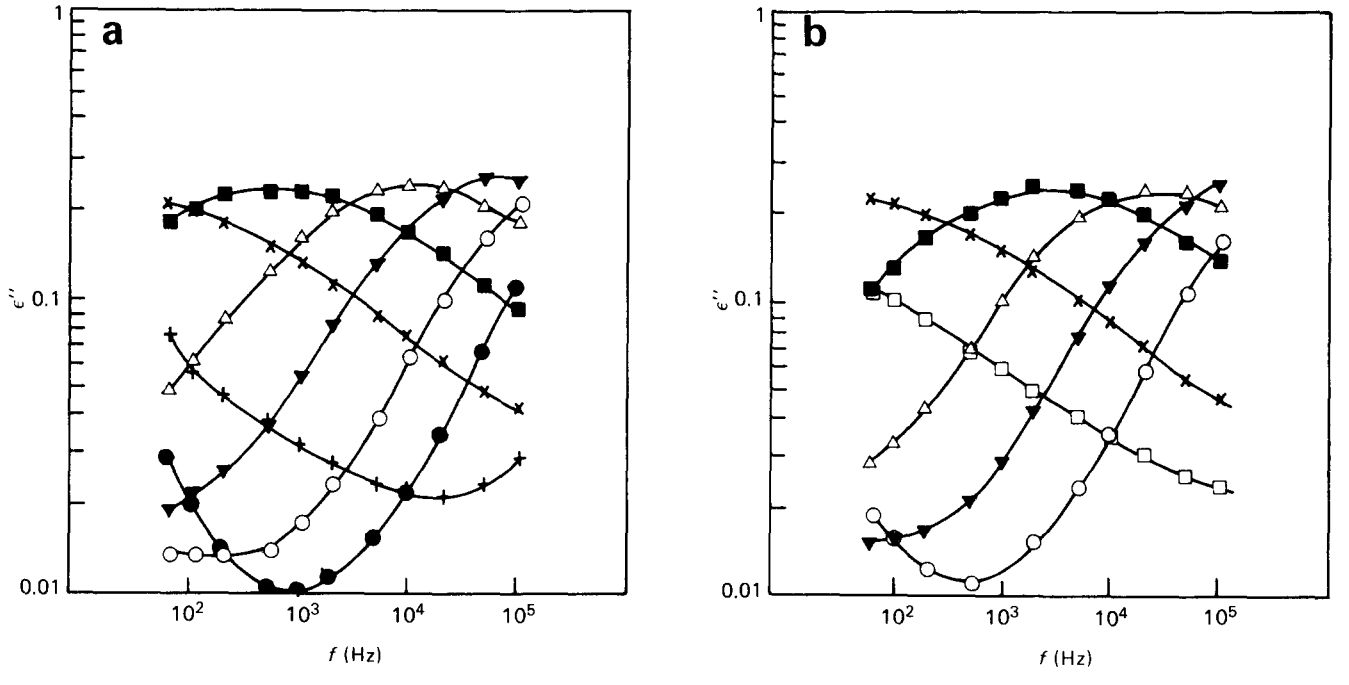

Figure 5 Dielectric relaxation spectrum ε'' vs. $\log(f)$: (a) (+) $T = 15.5$°C, (×) $T = 24.9$°C, (■) $T = 34.9$°C, (▲) $T = 44.8$°C, (▼) $T = 54.6$°C, (○) $T = 64.6$°C, (●) $T = 74.5$°C; (b) (□) $T = 20.4$°C, (×) $T = 29.9$°C, (■) $T = 39.8$°C, (▲) $T = 49.5$°C, (▼) $T = 59.6$°C, (○) $T = 69.4$°C

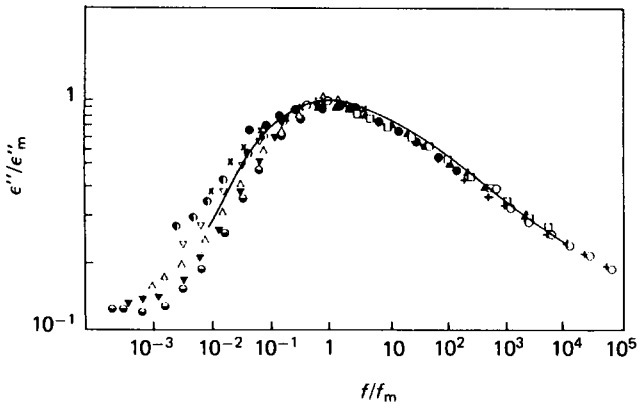

Figure 6 Master curve $\log(\varepsilon''/\varepsilon''_m)$ vs. $\log(f/f_m)$. The full curve is the curve calculated with the William–Watts model with $\beta = 0.35$. Points: (○) $T = 15.5$°C, (+) $T = 20.4$°C, (□) $T = 24.9$°C, (▲) $T = 29.9$°C, (●) $T = 34.9$°C, (×) $T = 39.8$°C, (◐) $T = 44.8$°C, (▽) $T = 49.5$°C, (△) $T = 54.6$°C, (▼) $T = 59.6$°C, (◒) $T = 64.6$°C

when the temperature decreases, with smaller values of the configurational entropy.

An equilibrium second-order transition is predicted when the configurational entropy vanishes, at temperature T_2 (ref. 30). Nevertheless this equilibrium transition is not experimentally attainable because, when the temperature decreases from well above T_2, the time required for the conformational rearrangements increases as the number of available states for the polymer decreases. This takes the material out of thermodynamic equilibrium. The transition to the glassy state takes place at a temperature about 50°C above the theoretically predicted T_2, when a critical value of the probability of conformational changes is attained. This probability also controls the viscoelastic or dielectric main relaxation process in amorphous polymers and its dependence on temperature, and yields the characteristic WLF behaviour of the viscoelastic and dielectric mean relaxation times[24,31].

In PBLG, the partition configurational function should be mainly determined around room temperature by the number and energy of the possible conformations of the side chains, since no conformational changes in the α-helices have been detected in this range of temperatures[8,32].

At high temperatures the number of states available to the material is high, the interaction between close chains being small. As the temperature decreases, the inter-helix distance diminishes[7]. The number of ways of packing the side chains together decreases because of this proximity, and thus the probability of conformational changes decreases. The process leading to the glass transition can be understood analogously to what happens in amorphous polymers.

When an electric field is applied to the material, the orientation of the permanent dipole of the COO group is produced by means of conformational rearrangements of the side chains, and the dielectric relaxation times are also governed by the probability of those rearrangements leading to WLF behaviour.

The value of the β parameter, which defines the width of the structural and dielectric relaxations, supports the same molecular origin for both processes. The differences found in the values of the equilibrium recovery time, also encountered in amorphous polymers, have not been explained so far.

CONCLUSIONS

The PBLG exhibits, around ambient temperature, a structural relaxation process that is characteristic of a glass transition similar to that found in amorphous materials. The structural relaxation process has been characterized using the Adam–Gibbs–Vogel (AGV) phenomenological model, showing a behaviour very similar to that of amorphous polymers. The T_g determined by d.s.c. is ~26°C. A dielectric relaxation appears at temperatures above T_g. The parameter characterizing the width of the dielectric relaxation in the Williams–Watts model is similar to the one which determines the width of the recovery time distribution in the structural relaxation process. Both relaxation processes are ascribed to conformational rearrangements of the side chains in the inter-helix space.

ACKNOWLEDGEMENTS

We gratefully acknowledge Professor T. Nakagawa, who kindly supplied the polymer used in this paper. We thank the personnel of the Chemistry Department of the UPV, where the i.r. measurements were carried out. This work was partially supported by the CAICYT Project Number 0493-84.

REFERENCES

1 Bamford, C. H., Elliott, A. and Hanby, W. E. 'Synthetic Polypeptides', Academic Press, New York, 1956
2 Miyazawa, T. in 'Poly α-Amino Acids' (Ed. G. D. Fasman), Marcel Dekker, New York, 1967, p. 69; Saludjian, P. and Luzzati, V. *ibid.* p. 157
3 Elliott, A., Fraser, R. D. and MacRae, T. P. *J. Mol. Biol.* 1965, **2**, 821
4 Watanabe, J., Imai, K., Gehani, R. and Uematsu, I. *J. Polym. Sci., Polym. Phys. Edn.* 1981. **19**, 653
5 McKinnon, A. J. and Tobolsky, A. V. *J. Phys. Chem.* 1966, **70**, 1453
6 McKinnon, A. J. and Tobolsky, A. V. *J. Phys. Chem.* 1968, **72**, 1157
7 Matsushima, N., Hikichi, K., Tsutsumi, A. and Kaneko, M. *Polym. J.* 1975, **7**, 44
8 Hikichi, K. *J. Phys. Soc. Japan* 1964, **19**, 2169
9 Mitsui, Y., Iitaka, Y. and Tsuboi, M. *J. Mol. Biol.* 1967, **24**, 15
10 Hikichi, K. *Rep. Prog. Polym. Phys. Japan* 1978, **21**, 509
11 Yamashita, Y., Tsutsumi, A., Hikichi, K. and Kaneko, M. *Polym. J.* 1975, **8**, 114
12 Tsutsumi, A., Hikichi, K., Takahashi, T., Yamashita, Y., Matsushima, N., Masahiro, K. and Kaneko, M. *J. Macromol. Sci.–Phys. (B)* 1973, **8** (3–4), 413
13 Takahashi, T., Tsutsumi, A., Hikichi, K. and Kaneko, M. *Macromolecules* 1974, **7**, 806
14 Matsushima, N., Hikichi, K., Tsutsumi, A. and Kaneko, M. *Polym. J.* 1975, **7**, 646
15 Gómez Ribelles, J. L., Diaz Calleja, R., Ferguson, R. and Cowie, J. M. G. *Polymer* 1987, **28**, 2262
16 Gómez Ribelles, J. L., Ribes Greus, A. and Diaz Calleja, R. To be published
17 Bauwens-Crowet, C. and Bauwens, J. C. *Polymer* 1986, **27**, 709
18 Narayanaswamy, O. R. *J. Am. Ceram. Soc.* 1971, **54**, 491
19 Moynhihan, C. T., Macedo, P. B., Montrose, C. J., Gupta, P. K., DeBolt, M. A., Dill, J. F., Dom, B. E., Drake, P. W., Easteal, A. J., Elterman, P. B., Moeller, R. P., Sasabe, H. and Wilder, J. A. *Ann. NY Acad. Sci.* 1976, **15**, 279
20 Hodge, I. M. *Macromolecules* 1987, **20**, 2897
21 Kovacs, A. J., Aklonis, J. J., Hutchinson, J. M. and Ramos, A. R. *J. Polym. Sci., Polym. Phys. Edn.* 1979, **17**, 1097
22 Williams, G. and Watts, D. C. *Trans. Faraday Soc.* 1970, **66**, 80
23 Chow, T. S. *Polym. Eng. Sci.* 1984, **24**, 1079
24 Adam, G. and Gibbs, J. H. *J. Chem. Phys.* 1965, **43**, 139

25 Berens, A. R. and Hodge, I. M. *Macromolecules* 1982, **15**, 756
26 Nedler, J. A. and Mead, R. *Comput. J.* 1965, **7**, 308
27 Tribone, J. J., O'Reilly, J. M. and Greener, J. *Macromolecules* 1986, **19**, 1732
28 Prost, W. M., Roberts, F. J. and Hodge, I. Proceedings of the 12th NATAS Conference, Sept. 1980, Williamsburg, VA, p. 119
29 Williams, G., Watts, D. C., Dev, S. B. and North, A. M. *Trans. Faraday Soc.* 1971, **67**, 1323
30 Gibbs, J. H. and DiMarzio, E. A. *J. Chem. Phys.* 1958, **28**, 373
31 Bueche, F. *J. Chem. Phys.* 1956, **24**, 418
32 Kuroishi, M., Kajiyama, T. and Takayanagi, M. *Chem. Lett.* 1973, 659